24th INTERNATIONAL CONGRESS ON SOUND AND VIBRATION
23–27 July 2017, London

ICSV24
23-27JULY 2017
LONDON CALLING

LOW FREQUENCY GENERATION, TRANSMISSION AND REFLECTION OF DIRECT AND INDIRECT PERTURBATIONS THROUGH NOZZLES

Simone Hochgreb, Erwan O. Rolland, Francesca De Domenico,
University of Cambridge, Department of Engineering, Cambridge, UK
email: simone.hochgreb@eng.cam.ac.uk

Pressure perturbations arise in combustors from direct noise related to the change in density in flames, as well as the indirect (entropic) noise associated with the acceleration of non-homogeneous regions of flow through nozzles. In this paper we review our recent work on quantifying the relative contributions of direct and indirect noise generated from perturbations in temperature and composition, and the resulting transmitted and reflected pressure perturbations. We show that (a) isentropic models are inadequate to capture the acoustic and entropic transfer functions across a nozzle; (b) corrections to non-isentropic behaviour are possible using existing models for orifices using a single parameter accounting for losses; (c) the behaviour of low frequency entropic noise generated in a chamber can be entirely accounted for when reverberation is taken into account; and (d) indirect noise due to compositional fluctuations can be as large as entropic noise arising from temperature fluctuations. The findings have implications for both the study of entropy noise in model systems, as well as for understanding how to separate the origins of noise in practical systems. In particular, the role of compositional noise in gas turbines (regarding for example the role of cooling in rich-quench-lean turbines) and the role of non-isentropic effects is not accounted for in current models, and should be revisited in the light of current findings.
Keyword: thermoacoustics, entropy noise, reverberation, combustion

1. Introduction

The role of acoustic perturbations in combustion devices is a topic of increasing interest, particularly as a source of potential instabilities. Acoustic waves are classified as direct and indirect noise. The former arises directly from the heat release rate perturbations in the flame. The latter is generated indirectly from the acceleration of regions of non-uniform temperature, density, composition or vorticity through narrow passages such as turbine nozzle guide vanes. Once created, these acoustic waves (direct and indirect noise) travel through the combustion chamber at the relative speed of sound, until they reach a boundary, where part of their energy is reflected, transmitted and absorbed. Temperature fluctuations have received most of the attention, but other sources of indirect noise may also play an important role.

A number of investigators have tackled the theoretical problem using one-dimensional Linearised Euler Equations (LEEs) based on linear perturbations impinging on a compact nozzle (i.e. for low-frequency perturbations). Marble and Candel [1] originally derived transfer functions for the acoustic waves generated by impinging entropy or acoustic perturbations in the low frequency limit, followed by works to account for different nozzle geometries [2, 3, 4], as well as non-linear perturbations [5, 6], and arbitrary nozzle shapes and frequencies [7]. A recent review tackles the recent progress in understanding and modeling entropy noise associated with temperature fluctuations [8], and a recent paper introduces the concept of noise produced by composition fluctuations [9].

Experimental investigations of indirect noise have proved to be difficult. Specifically, separating the contributions of direct and indirect noise is challenging, as these tend to be highly correlated,

and hard to distinguish, particularly in the noisy environment of a combustor [10, 11]. A popular means to circumvent these difficulties is to carry out simplified experiments, in which entropy noise is generated artificially, using a synthetic source such as an electric heater rather than a flame [12, 13], or mass injection for composition fluctuations [14].

Early attempts [15] showed that the main limitation to synthetic hot spot generation by pulsating an electric heater is the slow time response of heating meshes, but several experimental rigs now exist based on this initial idea [12, 16, 17]. The hot spots are allowed to convect through a converging-diverging nozzle, which can be operated both in the subsonic an supersonic regimes.

The DLR entropy wave generator experiment led to several efforts to explain its results analytically and numerically [18, 19, 20, 21, 22, 23]. However, difficulties with characterizing the transmission characteristics of the boundary conditions, possibly associated with the use of instrumentation with poor response at the very low frequencies of operation [13], limited the use of the data for validation.

Our recent experiments at Cambridge were designed to overcome the original difficulties with the DLR experiments by carefully tailoring and measuring the duct transmission characteristics, so as to allow for either anechoic conditions, and/or an appropriate accounting of the multiple reflections of the direct and indirect noise through well defined boundaries in the system in order to offer an unambiguous and quantitative measure of direct and indirect noise arising from synthetic perturbations of thermal energy, mass injection or compositional fluctuations. The work is detailed [24, 14, 13, 25] and in other papers in this conference (557,746).

2. Generalised transfer functions

The general flow conditions can be represented as a duct with generally variable cross sectional area, and arbitrary boundary conditions which can be controlled over the time scale of the experiment from anechoic, a pressure node or a pressure anti-node, through which passes a given flow with a specified conditions, as shown in Fig. 1. An excitation source (wave generator) creates direct acoustic pressure waves (π_d^-, π_d^+) propagating downstream (+) or upstream (-), and entropic (σ) and compositional (ξ) disturbances convected with the flow. Indirect acoustic waves (π_i^-, π_i^+) are subsequently generated at a nozzle further downstream. Upstream and downstream boundary conditions can be varied. The system mimics a combustor or any other device where energy, mass or compositional fluctuations can arise.

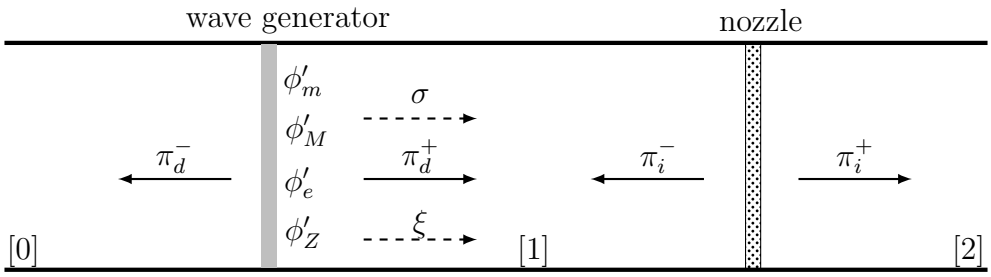

Figure 1: Direct acoustic (π_d^-, π_d^+), entropic (σ) and compositional (ξ) waves produced at a wave generator, and indirect acoustic waves (π_i^-, π_i^+) subsequently generated at a nozzle further downstream. Upstream and downstream boundary conditions can be varied.

The wave amplitudes are given by:

$$\pi^{\pm} \equiv \frac{1}{2}\left(\frac{p'}{\gamma\bar{p}} \pm \frac{u'}{\bar{c}}\right), \qquad \sigma \equiv \frac{s'}{\bar{c_p}}, \qquad \xi \equiv Z' \tag{1}$$

where p is the pressure, u is the flow velocity, c is the sound speed, s is the specific entropy, c_p is the specific heat capacity, γ is the heat capacity ratio, and Z is the mixture fraction.

The perturbations of mass, momentum, energy and concentration produced at the wave generator are defined as:

$$\varphi'_m = \frac{\phi'_m}{\bar{\rho}\bar{u}} \qquad \varphi'_M = \frac{\phi'_M}{\bar{\rho}\bar{u}^2} \qquad \varphi'_e = \frac{\phi'_e}{\bar{\rho}\bar{u}c_p\bar{T}} \qquad \varphi'_Z = \phi'_Z. \tag{2}$$

where ϕ'_m, ϕ'_M, ϕ'_e and ϕ'_Z are the changes in mass, momentum, energy and composition respectively. Conservation equations for these same quantities connect the direct noise perturbations in upstream and downstream pressure, entropy and composition. Indirect noise is generated from entropic (σ) and compositional (ξ) fluctuations in the flow. We can organize a system of equations connecting the source of the perturbations $\boldsymbol{\varphi} = [\varphi'_m, \varphi'_M, \varphi'_e, \varphi'_Z]$ at the wave generator or the acceleration at the nozzle to the resulting perturbations $\boldsymbol{\pi_d} = [\pi_d^+, \pi_d^-, \sigma, \xi]$ across the wave generator, via a transfer function for the wave generator $\mathbf{T_w}$ as:

$$\boldsymbol{\pi_d} = \mathbf{T_w}\boldsymbol{\varphi} \tag{3}$$

Again, conservation equations described in [7], [1], [9] and [14] connect the magnitude of these perturbations to the indirect noise $\boldsymbol{\pi_i} = [\pi_i^+, \pi_i^-]$

$$\boldsymbol{\pi_i} = \mathbf{T_i}\boldsymbol{\pi_d} = \mathbf{T_i}\mathbf{T_w}\boldsymbol{\varphi} \tag{4}$$

Finally, the waves generated are reflected and/or transmitted at the boundaries of the system via reflection, transmission and dissipation coefficients at the boundaries. One can therefore generalise the equations for the up- and downstream waves in the form of transfer functions for the acoustic saves $\boldsymbol{\pi} = [\pi_d^+, \pi_d^-, \pi_i^+, \pi_i^-]$ as a function of the input perturbations can be solved in either the time or frequency domain according to a generalized transfer matrix for the pressure contribution of each of the components, or as the sum of all contributions:

$$\boldsymbol{\pi} = \mathbf{T}\boldsymbol{\varphi} \tag{5}$$

Finally, by using transfer functions $\boldsymbol{\mathcal{R}}$ based on the upstream and downstream reflection coefficients, it is possible to solve the equations for the contributors for the total local pressure formed by the components in $\boldsymbol{\pi}$ for comparison with experiments:

$$\frac{p'}{\gamma\bar{p}} = \boldsymbol{\mathcal{R}}\boldsymbol{\pi} = \boldsymbol{\mathcal{R}}\mathbf{T}\boldsymbol{\varphi} \tag{6}$$

This framework allows us to experiment with systems with arbitrary boundary conditions, so that it is possible to isolate the contribution of direct and indirect noise from the elements in the matrix in time or by changing the boundaries and reflection coefficients. The details of the transfer matrices and how the reflection coefficients can be found in the respective papers, and in the highlighted sections below.

3. Experimental setup

The details of the experimental setup are detailed in [24, 14, 13, 25] and in papers (557,746). The device, dubbed the Cambridge Entropy Generator (CEG) can be described as follows. Air flows through a 42.6 mm diameter tube, delimited by a mass flow controller for filtered air (Alicat MCR500 or MCR250, $\pm$ 1% full scale) at the upstream end, and nozzles of variable area and shape at the downstream end. The heat, mass and compositional perturbations are generated as follows: (a) heat release rate perturbations are created using a pulsed electrical source generating around 400 W over hundreds of milliseconds, which delivers power to micron-diameter wire grids, corresponding to a

maximum temperature rise of the order of 20 K from ambient temperature, (b) mass and compositional perturbations are generated by injecting air or helium gas corresponding to a few percent of the mass of the total flow rate over a few hundreds of milliseconds. In either case, the perturbations are limited to below 10 Hz frequency owing to limitations associated with the cooling of the wires for the heating, or the duty cycle of the valves for mass injection.

The boundary conditions are controlled as follows: the upstream boundary is controlled by a mass flow controller and a transfer duct, which operates as a pressure antinode. The downstream boundary can be controlled either using a variety of converging nozzle terminations into the atmosphere, as well as shaped convergent-divergent nozzles with very long terminations (60 m) for anechoic conditions. These are described in [25].

Static and dynamic pressures are measured using flush mounted Kulite XT-140M and XT-190M piezoresistive transducers at suitable points along the ducts to interpret the acquired pressure trace during the perturbations. The transducer signals are amplified using a Flyde FE-379-TA amplifier, and acquired using a NI-2090 DAQ box connected to a NI PCI-5259 card. The signal is sampled at 8192 Hz with a 16-bit resolution. These signals can be averaged or single shot, as needed from different types of experiments.

4. Results

4.1 Low frequency entropy noise and reverberation

Many of the previous models have tacitly adopted the isentropic models for entropy generation. In the absence of available experimental data for cross-checking, there has been no challenge to existing models. The difficulties in matching experimental and modelled results regarding the DLR experiments [18, 19, 20, 21, 22, 23] highlighted the particular importance of characterising the effect of the boundary conditions: the very low frequency of the experiments means that pressure waves arising from either direct or indirect noise have a chance to reflect multiple times during and after the heating pulse, building up the pressure wave. This is illustrated in Fig. 2 : the black line represents the pressure trace for a fully anechoic case, and the blue line the experimental measurement case for the reverberating chamber. Clearly the pressure achieved in the case of the experiment is at odds with the theory, and the effect of the multiple wave addition must be taken into account. Rolland *et al.* [24] have proposed and tested a detailed theory of reverberating noise for the purpose, showing that it is possible to develop a model for the reverberation of direct and indirect noise in the duct, based on the measured acoustic reflection coefficients, which captures the behaviour of the observed pressure with good accuracy. Figure 3 and the analysis in the paper show that the behavior of the direct noise with the pressure rising during the heating pulse can be captured after adding the reflection coefficient obtained from the theory of non-isentropic nozzles [26], as described in the next subsection. The magnitude of the indirect noise predicted from isentropic formulation [1], which appears as a negative pulse (which moves quicker as the convection increases), is smaller than experimentally measured, even after accounting for reverberation. This requires a correction to the entropic noise generated by the non-isentropic nozzle, as addressed in the next subsection.

4.2 Non-isentropic nozzles

Preliminary experiments the CEG were conducted using reflecting boundaries (an acoustically closed upstream end and subsonic or sonic nozzles) enclosing the entropy generator [13, 24]. The experiments showed that by using a suitably large distance between the entropy generator and the nozzle, it was possible to clearly separate the contributions of the direct and indirect noise in the overall upstream propagating noise, as illustrated in Fig. 2 for the reverberating cavity. Originally, the experiment was done using orifice plates. Later on, De Domenico *et al.* [25] replicated the same experiment using different converging-nozzles and showed that the shape and angle of the convergence

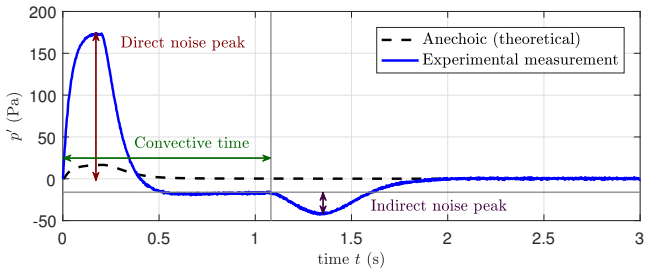

Figure 2: Acoustic pressure fluctuation history for duct velocity $U = 0.88m/s$ in the subsonic long-tube (1.4 m) configuration. Experimental measurement (solid line), analytical result with no acoustic reflections ($R_1 = R_2 = 0$) (dashed line). Direct noise appears during the first 0.2 s as heating is on, indirect noise appears after 1 s, as a negative pulse.

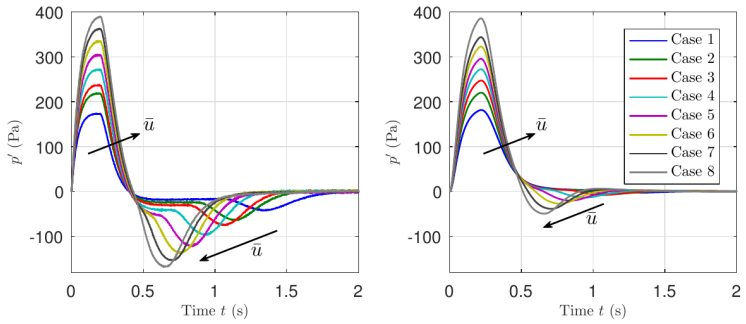

Figure 3: Acoustic pressure fluctuation histories for variable duct velocities from 0.88 to 2.56 m/s in a subsonic long-tube (1.4 m) terminated by an orifice. Modified from [24]. Left: experiments. Right: simulations.

do not affect the generation of upstream-propagating entropy noise π_i^- for such low frequencies.

In order to model the experimental results, the acoustic and entropic transfer functions of the nozzle need to be accounted for in the reverberation model. Many of the previous models and simulations have adopted the isentropic assumption, which implies that no pressure losses occur within the nozzle. In real situations, however, this may not be the case: losses and recirculation zones often appear across nozzles if the diverging ratio is not very small, so that the flow is not isentropic. The non-isentropicity is taken into account in existing models for the acoustic reflection coefficients [27, 26]. However, no analytical formulations on the entropy-to-sound conversion in non-isentropic boundaries had been available in the literature.

The paper by Rolland *et al.* [24] considered both the reverberation of the acoustic waves and the acoustic reflection coefficient for a non-isentropic nozzle by [27] and [26], to show that the acquired *direct* noise is well reproduced for a non-isentropic converging nozzle (Figs. 4 and 5). However, the measured magnitude of the entropy noise is significantly larger than predictions using the isentropic model (Fig. 4).

A further effort has been made by De Domenico *et al.* to address this discrepancy [28]. If the non-isentropic behaviour of the convergent nozzle is taken into account, the experimental indirect noise obtained from the orifice plate is correctly predicted, as shown in Fig. 5(b). Therefore, both for the direct and the indirect noise there is clearly excellent agreement between corrected models and experiments, showing that the experimental data is far from the isentropic case (Fig. 5).

The proposed corrections emphasize how non-isentropic formulations are required to correctly understand the acquired pressure traces in dissipative systems. In a recent paper, De Domenico *et al.* [28] measured the pressure perturbations generated by convergent-divergent nozzle terminations, and proposed a generalised model for non-isentropic jump conditions. The generalised transfer function builds on the analytical model of Durrieu *et al.* [26], incorporating an area ratio for momentum con-

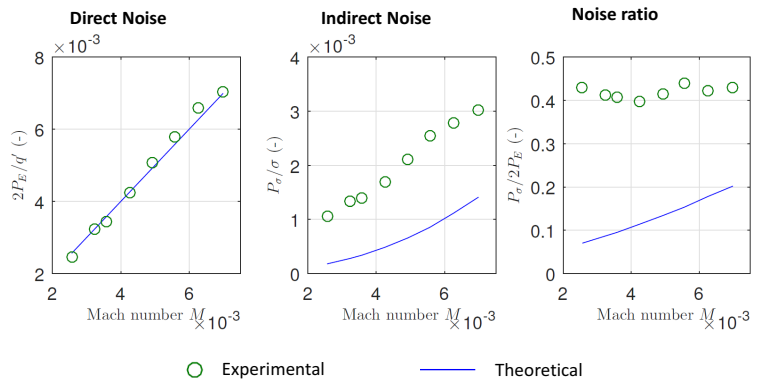

Figure 4: Decomposition of direct and indirect noise as a function of Mach number, and ratio of indirect to direct noise. Lines: isentropic model.

servation across the nozzle, which roughly corresponds to the area where separation effectively takes place: for an area ratio equal to unity relatively to the throat, the nozzle behaves as an orifice plate; for a detachment area corresponding to the downstream area, isentropic conditions are recovered.

Non isentropic results showed that for converging nozzles and even for slowly diverging nozzles, the acoustic and entropic transmissivity is low, and that for high Mach numbers, the convergent/divergent nozzle behaves nearly as a purely converging nozzle, *i.e.* the temperature fluctuation generates an acoustic wave which propagates upstream, but does not have a corresponding wave generated downstream. This accounts for the higher indirect noise than expected in Fig. 5, as the absence of the opposing wave in the diverging section means that the magnitude of the indirect acoustic wave is larger than the isentropic theory would indicate.

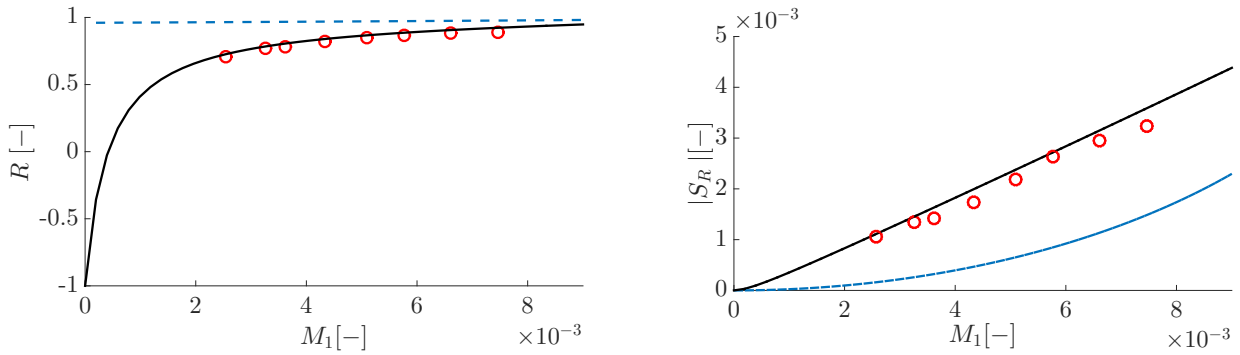

Figure 5: Acoustic (a) and entropic (b) reflection coefficients of the convergent-nozzle-duct termination [25][paper 557 in this conference]: experimental data (markers), isentropic predictions (blue lines) and generalised transfer function predictions (solid black lines).

4.3 Compositional noise

The recent suggestion of entropic compositional noise by Magri *et al.* [9] provided an opportunity to use the CEG for testing the theory of entropy noise generation via compositional fluctuations. The method used is that of injection of a different gas than air, and to use the same rationale of measuring the entropic noise via the corresponding time delay observed. The details of the derivation can be found in the original paper, but in general, the entropic disturbance can be decomposed into contributions from perturbations between relative energy per unit mass, momentum per unit mass or composition. By comparing the addition of perturbations of equal momentum per unit mass, and

equal energy per unit mass, it is possible to extract the entropy perturbation per unit mass composition difference.

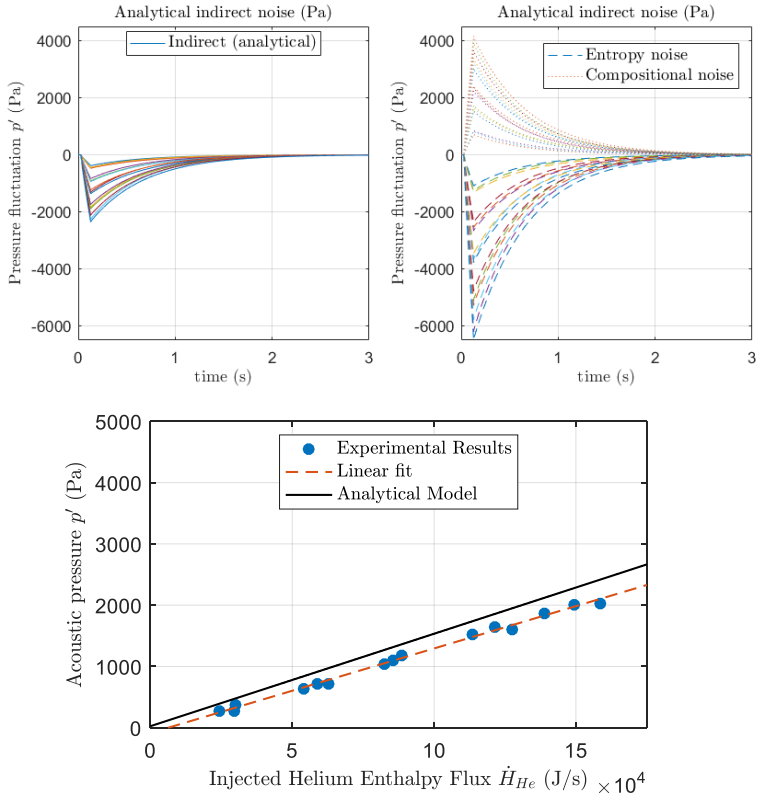

Figure 6: Top: Experimental and analytically reconstructed direct and indirect noise obtained from the injection of increasing mass flow rates of helium [14] Bottom: comparison of analytical and experimental composition noise.

5. Conclusions

The use of the CEG as modular experimental facility for testing acoustic and entropic model has revealed the successes and limitations of 1D perturbation models, by including reverberation. Most importantly, we have found that isentropic models are inadequate to capture the acoustic and entropic transfer functions across a nozzle, but that there are readily available non-isentropic models that can capture the behaviour of the direct acoustic noise. Further work is necessary to capture the behaviour of non-isentropic entropy generation ab initio. The indirect noise due to compositional fluctuations can be as large as entropic noise arising from temperature fluctuations. These adjustments have not been accounted for previously, and should be included in future entropy-to-sound models.

REFERENCES

1. Marble, F. and Candel, S. Acoustic disturbance from gas non-uniformities convected through a nozzle, *Journal of Sound and Vibration*, **55** (2), 225–243, (1977).
2. Moase, W. H., Brear, M. J. and Manzie, C. The forced response of choked nozzles and supersonic diffusers, *Journal of Fluid Mechanics*, **585**, 281, (2007).
3. Stow, S. R., Dowling, A. P. and Hynes, T. P. Reflection of circumferential modes in a choked nozzle, *Journal of Fluid Mechanics*, **467**, 215–239, (2002).
4. Goh, C. S. and Morgans, A. S. Phase prediction of the response of choked nozzles to entropy and acoustic disturbances, *Journal of Sound and Vibration*, **330** (21), 5184–5198, (2011).

5. Huet, M. and Giauque, A. A nonlinear model for indirect combustion noise through a compact nozzle, *Journal of Fluid Mechanics*, **733**, 268–301, (2013).
6. Huet, M. Nonlinear indirect combustion noise for compact supercritical nozzle flows, *Journal of Sound and Vibration*, **374**, 211–227, (2016).
7. Durán, I. and Moreau, S. Solution of the quasi-one-dimensional linearized Euler equations using flow invariants and the Magnus expansion, *Journal of Fluid Mechanics*, **723**, 190–231, (2013).
8. Morgans, A. S. and Duran, I., (2016), *Entropy noise: a review of theory, progress and challenges*.
9. Magri, L., O'Brien, J. and Ihme, M. Compositional inhomogeneities as a source of indirect combustion noise, *Journal of Fluid Mechanics*, **799**, R4, (2016).
10. Tao, W., Mazur, M., Huet, M. and Richecoeur, F. Indirect Combustion Noise Contributions in a Gas Turbine Model Combustor with a Choked Nozzle, *Combustion Science and Technology*, **188** (4-5), 793–804, (2016).
11. Becerril, C., Moreau, S., Bauerheim, M., Gicquel, L. and Poinsot, T. Numerical investigation of combustion noise: The Entropy Wave Generator, *22nd AIAA/CEAS Aeroacoustics Conference*, Reston, Virginia, may, American Institute of Aeronautics and Astronautics, (2016).
12. Bake, F., Richter, C., Mühlbauer, B., Kings, N., Röhle, I., Thiele, F. and Noll, B. The Entropy Wave Generator (EWG): A reference case on entropy noise, *Journal of Sound and Vibration*, **326** (3-5), 574–598, (2009).
13. De Domenico, F., Rolland, E. and Hochgreb, S. Detection of direct and indirect noise generated by synthetic hot spots in a duct [Accepted], *Journal of Sound and Vibration*, (2017).
14. Rolland, E. O., De Domenico, F. and Hochgreb, S. Direct and indirect noise generated by injected entropic and compositional inhomogeneities, *Proceedings of ASME 2017 Turbomachinery Technical Conference & Exposition GT2017 June 26-30, 2017, Charlotte, USA*, pp. GT2017–64428, (2017).
15. Bohn, M. S., *Noise produced by the interaction of acoustic waves and entropy waves with high speed nozzle flows*, Ph.D. thesis, California Insitute of Technology, (1976).
16. Hake, M. I., *Experimental Design to Determine the Effect of Temperature and Mach Number on Entropy Noise*, Ph.D. thesis, Massuachusets Institute of Technology, (2014).
17. De Domenico, F., Rolland, E. O. and Hochgreb, S. Detection of direct and indirect noise generated by synthetic hot spots in a duct, *Journal of Sound and Vibration*, pp. 1–17, (2017).
18. Mühlbauer, B., Noll, B. and Aigner, M. Numerical Investigation of the Fundamental Mechanism for Entropy Noise Generation in Aero-Engines, *Acta Acustica united with Acustica*, **95** (3), 470–478, (2009).
19. Howe, M. S. Indirect combustion noise, *Journal of Fluid Mechanics*, **659** (-1), 267–288, (2010).
20. Leyko, M., Moreau, S., Nicoud, F. and Poinsot, T. Numerical and analytical modelling of entropy noise in a supersonic nozzle with a shock, *Journal of Sound and Vibration*, **330** (16), 3944–3958, (2011).
21. Giauque, A., Huet, M. and Cléro, F. Analytical Analysis of Indirect Combustion Noise In Subcritical Nozzles, *ASME Turbo Expo 2012*, jun, (2012).
22. Durán, I., Moreau, S. and Poinsot, T. Analytical and Numerical Study of Combustion Noise Through a Subsonic Nozzle, *AIAA Journal*, **51** (1), 42–52, (2013).
23. Lourier, J. M., Huber, A., Noll, B. and Aigner, M. Numerical Analysis of Indirect Combustion Noise Generation Within a Subsonic Nozzle, *AIAA Journal*, **52** (10), 2114–2126, (2014).
24. Rolland, E. O., De Domenico, F. and Hochgreb, S. Theory and application of reverberated direct and indirect noise, *Journal of Fluid Mechanics*, (2017).
25. De Domenico, F., Rolland, E. O. and Hochgreb, S. Measurements of the Effect of Boundary Conditions on Upstream and Downstream Noise Arising from Entropy Spots, *Proceedings of ASME Turbo Expo 2017 GT2017*, (2017).
26. Durrieu, P., Hofmans, G., Ajello, G., Boot, R., Aurégan, Y., Hirschberg, A. and Peters, M. C. Quasisteady Aero-Acoustic Response of Orifices., *The Journal of the Acoustical Society of America*, **110** (4), 1859–1872, (2001).
27. Bechert, D. Sound Absorption Caused by Vorticity Shedding, Demonstrated with a Jet Flow, *Journal of Sound and Vibration*, **70** (79), 389–405, (1980).
28. De Domenico, F., Rolland, E. O. and Hochgreb, S. Acoustic and entropic transfer functions of a generalised subsonic nozzle, *Proceedings of the ICSV Conference 2017*, p. 557, (2017).